Cooperatively enhanced precision of hybrid light-matter sensors

Artur Niezgoda,[1] Jan Chwedeńczuk,[1] Tomasz Wasak,[2] and Francesco Piazza[2]
[1]*Faculty of Physics, University of Warsaw, ul. Pasteura 5, PL-02-093 Warszawa, Poland*
[2]*Max-Planck-Institut für Physik komplexer Systeme, 01187 Dresden, Germany*

(Received 5 January 2021; accepted 15 July 2021; published 19 August 2021)

We consider a hybrid system of matter and light as a sensing device and quantify the role of cooperative effects. The latter generically enhance the precision with which modifications of the effective light-matter coupling constant can be measured. In particular, considering a fundamental model of N qubits coupled to a single electromagnetic mode, we demonstrate that the ultimate bound for the precision shows double-Heisenberg scaling: $\Delta\theta \propto 1/(Nn)$, with N and n the number of qubits and photons, respectively. Moreover, even using classical states and measuring only one subsystem, a Heisenberg-times-shot-noise scaling, i.e., $1/(N\sqrt{n})$ or $1/(n\sqrt{N})$, is reached. As an application, we show that a Bose-Einstein condensate trapped in a double-well optical lattice within an optical cavity can in principle be used to detect the gravitational acceleration g with the relative precision of $\Delta g/g \sim 10^{-4}\ \mathrm{Hz}^{-1/2}$. The analytical approach presented in this study takes into account the leakage of photons through the cavity mirrors, and allows one to determine the sensitivity when g is inferred via measurements on atoms or photons.

DOI: 10.1103/PhysRevA.104.023315

I. INTRODUCTION

The use of hybrid light-matter systems has a large potential for the development of classical and quantum technologies. The idea of exploiting the best of both worlds culminates in the concept of a quantum network [1–3], where photons act as information carriers channeling between nodes, while the matter is used for information storage and as source of the nonlinearities needed for information processing. These optical nonlinearities correlate matter with light, allowing one to gain information and even modify the former by measuring the latter. This permits one, for instance, to control the motion of mechanical objects via light in optomechanical systems [4,5], with important consequences for interferometry of displacement measurements [6–11].

For such schemes it is crucial to reach a strong light-matter coupling, which can be achieved by employing optical resonators. Among the most promising kinds of matter, neutral atoms stand out due to the high control achievable over internal and external degrees of freedom [12–14]. For instance, atom-light coupling can generate the entanglement between the two subsystems [15–21] or be exploited to efficiently create entanglement in atomic ensembles [22–35]. This constitutes an alternative route to the use of intrinsic atom-atom nonlinearities [36–46], with applications for quantum metrology beating the shot-noise limit [47–49]. Hybrid devices exploiting atom-light nonlinearities and cooperative effects for metrology and sensing include white-light interferometers with anomalous dispersion [50,51], superradiance [52] and superradiant lasers [53,54], single-atom cavity-QED platforms for nonclassical light [55], quantum statetransfer protocols with information recycling [56–59], and optical magnetometers [60,61] and their nonlinear version [62]. In particular, in the field of inertial sensing with atoms [63–67], the use of optical resonators has been shown to enhance the precision of a Mach-Zehnder interferometer [68] and is, for instance, expected to improve the sensitivity of Bloch-oscillation-based metrology [69,70]. More recently, the supersolid phase of ultracold bosons induced by the coupling to an optical resonator has been predicted to allow for very precise gravimetry [71,72]. Also, an optical cavity-QED setting with strong cooperative atom-light interactions has been used to create nonclassical states of light, which allow for electric-field sensing beyond the standard quantum limit [73]. Despite these various applications, a systematic study of the performance of hybrid light-matter systems is still lacking in the regime where cooperative effects are dominant.

In this work, we characterize the different working regimes of a hybrid light-matter sensor aiming at measuring modifications of the effective light-matter coupling constant. We consider a minimal model for cooperative effects, consisting of N qubits coupled to a single electromagnetic mode. This model allows for closed analytical expressions for the measurement error, also called the precision or the sensitivity. We find that the ultimate bound for the error satisfies a double-Heisenberg scaling: $\Delta\theta \propto 1/(Nn)$, with both the number of qubits N and of photons n. We also study the dependence on different initial states (classical and nonclassical) of the system, as well as on different measurements. Even for classical states of qubits and photons, and by simply measuring a qubit or a photon observable, the error scales partially at the Heisenberg limit, i.e., $\Delta\theta \propto 1/(\sqrt{N}n)$ or $\Delta\theta \propto 1/(N\sqrt{n})$, respectively.

Finally, we consider a specific example where an atomic Bose-Einstein condensate trapped in a double-well optical lattice is dispersively coupled to a single mode of an optical

 ©2021 American Physical Society

cavity. The gravitational acceleration g modifies the effective atom-photon coupling and this effect is amplified by the cooperative effects. We determine the dynamics of the system and analytically calculate the precision assuming that g is deduced either from the homodyne detection of the mean of the quadrature of light or from the mean imbalance between the atomic occupation of each well. We show that the relative error $\Delta g/g$, which scales inversely both with the numbers of atoms and photons, can in principle reach the level of 10^{-4} Hz$^{-1/2}$ with realistic parameters and classical states of matter and light, also including the effect of photon loss. Our results can be easily extended to other input states, regimes of parameters, or estimation protocols.

The paper is organized as follows: In Sec. II we introduce the model and derive the ultimate bounds for the sensitivity, as well as specific bounds for certain types of measurements and input states. In Sec. III we consider a specific scheme where the electromagnetic field is coherently driven and lossy and the qubits are prepared in a Gaussian state. In Sec. IV we present an application of our model in gravity sensing and its possible precision using coherent atomic states. We conclude in Sec. V. Detailed analytical calculations are presented in the Appendices.

In this work, the numerical calculations were performed by using a solver in-built in QuTip library, solving Schrödinger equations for noiseless case and a master equation with the photon losses included [74].

II. MODEL AND GENERAL PRECISION BOUNDS

In order to demonstrate how cooperative effects can enhance the sensitivity of a hybrid light-matter sensor we consider a minimal model describing N qubits all equally coupled to a single mode of an electromagnetic field, corresponding to the following Hamiltonian (for details, see Ref. [75] and Sec. IV):

$$\hat{H} = (-\Delta_c + c_1 N)\hat{n} + \eta(\hat{a} + \hat{a}^\dagger) + c_2\hat{n}\hat{J}_x, \tag{1}$$

where in the rotating frame Δ_c is the characteristic frequency of the electromagnetic mode which is coherently driven with a strength η, $\hat{n} = \hat{a}^\dagger\hat{a}$ is the number of photons in the mode, and $\hat{J}_x = \frac{1}{2}\sum_{i=1}^{N}\hat{\sigma}_x^{(i)}$ is the x component of the collective spin operator ($\hat{\sigma}_x^{(i)}$ is the x-axis Pauli matrix for the ith qubit). The Hamiltonian from Eq. (1) contains two types of light-matter coupling: a static collective shift of the electromagnetic mode frequency quantified by the coupling constant c_1, and a cavity-induced "quantized effective magnetic field" coupled to the collective spin operator (or, equivalently, a qubit-induced dynamical shift of the mode frequency) with characteristic strength c_2. Note that we set $\hbar = 1$ throughout the text.

A. Ultimate bounds on the sensitivity

We now demonstrate that the system governed by the Hamiltonian from Eq. (1) can be employed as a sensor for the estimation of a parameter θ entering the light-matter coupling constants c_1 and/or c_2, with the best possible precision showing the double-Heisenberg scaling $\Delta\theta \propto n^{-1}N^{-1}$, where $n = \langle\hat{n}\rangle$ is the number of photons.

To this end, we recall that according to the Cramer-Rao lower bound [76], the sensitivity in estimating the value of θ is bounded from below by

$$\Delta\theta \geqslant \frac{1}{\sqrt{F_Q}}. \tag{2}$$

Here F_Q is the quantum Fisher information (QFI) [77] given by

$$F_Q = \sum_{i,j}\frac{(\lambda_i - \lambda_j)^2}{\lambda_i + \lambda_j}|\langle i|\hat{h}|j\rangle|^2, \tag{3}$$

where $|i\rangle$'s and λ's are the eigenvectors and the corresponding eigenvalues of the density matrix, i.e., $\hat{\varrho} = \sum_i \lambda_i|i\rangle\langle i|$. For pure states, when only one λ is nonzero, this simplifies to

$$F_Q = 4(\langle\hat{h}^2\rangle - \langle\hat{h}\rangle^2) \equiv 4\langle(\Delta\hat{h})^2\rangle, \tag{4}$$

where the expectation values are calculated with the state $|\psi\rangle = \hat{U}|\psi_0\rangle$ transformed by the evolution operator $\hat{U} = e^{-i\hat{H}t}$. The operator $\hat{h}$ generates the Schrödinger-like transformation in the parameter space, namely,

$$\begin{aligned} i\partial_\theta|\psi\rangle &= i\partial_\theta\hat{U}|\psi_0\rangle = i(\partial_\theta\hat{U})\hat{U}^\dagger\hat{U}|\psi_0\rangle \\ &= i(\partial_\theta\hat{U})\hat{U}^\dagger|\psi\rangle = \hat{h}|\psi\rangle \end{aligned} \tag{5}$$

hence $\hat{h} = i(\partial_\theta\hat{U})\hat{U}^\dagger$ [77]. It can be rewritten in a more useful form (see Appendix A), namely,

$$\hat{U}(t) = \hat{D}^\dagger(\hat{\beta})e^{-i\hat{\omega}t\hat{a}^\dagger\hat{a}}\hat{D}(\hat{\beta})e^{i\eta t\hat{\beta}}, \tag{6}$$

where $\hat{\beta} = \eta\hat{\omega}^{-1}$ and $\hat{\omega} = -\Delta_c + c_1N + c_2\hat{J}_x$, and $\hat{D}(\hat{\beta}) = e^{\hat{\beta}\hat{a}^\dagger - \hat{\beta}^\dagger\hat{a}}$ is a generalization of the displacement operator [78,79]. With Eq. (6), the operator $\hat{h}$ can be evaluated explicitly (see Appendix B for details):

$$\begin{aligned} \hat{h} = \frac{\partial\hat{\omega}}{\partial\theta}\bigg(&- i\frac{\hat{\beta}^2}{\eta}(\hat{a}^\dagger - \hat{a}) + t(\hat{a}^\dagger + \hat{\beta})(\hat{a} + \hat{\beta}) \\ &+ i\frac{\hat{\beta}^2}{\eta}[(\hat{a}^\dagger + \hat{\beta})e^{it\hat{\omega}} - (\hat{a} + \hat{\beta})e^{-it\hat{\omega}}] + t\hat{\beta}^2\bigg). \end{aligned} \tag{7}$$

A large QFI and thereby a high sensitivity, is achieved whenever $\hat{h}$ scales strongly, i.e., at least linearly, with the number of particles and the time t. This is the case for the generator in Eq. (7), which contains terms scaling linearly with the number of qubits and photons, as well as with time t. To see it, we rewrite $\hat{h}$ as

$$\hat{h} = t\frac{\partial\hat{\omega}}{\partial\theta}\hat{a}^\dagger\hat{a} + \hat{f}(\hat{\omega}, \eta, \hat{a}, \hat{a}^\dagger; t), \tag{8}$$

where the explicit form of $\hat{f}$ can be read out from Eq. (7). In the absence of the drive, $\hat{f}$ is zero. In such a case, for a light-matter state

$$|\psi\rangle = \frac{\left|-\frac{N}{2}\right\rangle + \left|\frac{N}{2}\right\rangle}{\sqrt{2}} \otimes |n\rangle, \tag{9}$$

which is composed of a superposition of eigenstates of $\hat{J}_x$ with the minimal and the maximal eigenvalues (N-qubit cat state) and a photon Fock state, we obtain

$$F_Q = t^2c_2'^2n^2N^2, \tag{10}$$

i.e., a Heisenberg scaling with both the number of qubits and photons [80]. Here and below, primes denote the derivatives of coefficients of the Hamiltonian (1) over the parameter θ. The double-Heisenberg scaling of the QFI in (10) is a consequence of cooperative effects which can be understood as follows. A standard linear interferometer acting on a collection of qubits is generated by the operator $c_2\hat{J}_x$ and in this case, the maximal attainable sensitivity is

$$F_Q = t^2 c_2'^2 N^2. \tag{11}$$

In our situation, taking a photon Fock state $|n\rangle$, the term proportional to c_2 in the Hamiltonian from Eq. (1) is $c_2 n\hat{J}_x$. It is this additional coefficient n that yields the double-Heisenberg scaling in Eq. (10). Cooperative effects are present and enhance the sensitivity even using classical states of light and nonentangled states of the qubits at the input.

Let us consider the tensor product of a coherent state of light $|\alpha\rangle$ and a coherent state of qubits, i.e., a state where all qubits point in the z direction:

$$|\psi_A\rangle = \sum_{m=-N/2}^{N/2} C_m|m\rangle, \quad C_m = \frac{1}{2^{N/2}}\sqrt{\binom{N}{\frac{N}{2}\pm m}}, \tag{12}$$

where the sign $\pm$ depends on the choice of the direction along z and C_m's are the coefficients of the state in the basis of the eigenstates $|m\rangle$ of $\hat{J}_x$. For this state we have $\langle \hat{J}_x\rangle = 0$ and $\langle \hat{J}_x^2\rangle = \frac{N}{4}$, thus

$$F_Q = nt^2[4\varphi'^2 + (c_2')^2 N(n+1)], \tag{13}$$

where $n = |\alpha|^2$ and

$$\varphi = -\Delta_c + c_1 N. \tag{14}$$

Though the QFI from Eq. (13) is missing the double-Heisenberg scaling of Eq. (10), it still shows a Heisenberg scaling with the number of qubits (since φ scales with N) together with shot-noise scaling with the number of photons, or vice versa. The fact that this happens also using nonentangled input states tells us that the Heisenberg scaling in this case is a classical cooperative effect where the dynamics in the estimation-parameter space is accelerated by a factor proportional to the number of qubits or photons. An equivalent mechanism enhances the sensitivity of nonlinear interferometers [62].

Finally, to go beyond the scaling $N^2 n$ or Nn^2 with initially uncorrelated pure states of matter and light, and reach the double-Heisenberg scaling, when the QFI scales as N^2n^2, the state requires to be at least entangled in qubit or nonclassical (i.e., having a nonclassical distribution into the overcomplete basis of coherent states [81,82]) in photonic degrees of freedom. In the former case, the QFI contains the term $\langle(\Delta\hat{J}_x)\rangle n^2$, which yields the desired precision if the variance of the collective spin operator scales with N^2. With the nonclassical photonic states, in the QFI the dominating term is $(c_1'N + c_2'\langle\hat{J}_x\rangle)^2\langle(\Delta\hat{n})^2\rangle$, which leads to very high precision if the variance of the photonic distribution scales with n^2.

B. Bounds for specific measurements

Having found favorable scaling bounds for the sensitivity, one has to determine which estimation strategies—that is, which measurement observables and data processing protocols—saturate those bounds.

In this section, we address this issue by considering the case where the electromagnetic field is not driven. This simpler case is generalized to the driven-dissipative case in the next section. We specifically consider the bound given by Eq. (13), which corresponds to the uncorrelated light-matter input state of photonic coherent state $|\alpha\rangle$ (with the mean number of photons $n = |\alpha|^2$) and the coherent state of qubits given in Eq. (12).

We first consider the case where the measurement is performed on the qubits with the photonic degree of freedom traced out; specifically, the z component of the collective spin operator. The simplest estimation strategy is to deduce θ from the mean value of the measurements of $\hat{J}_z$. It gives the well-known error propagation formula for the sensitivity

$$\Delta^2\theta = \frac{\Delta^2\hat{J}_z}{\left(\frac{\partial\langle\hat{J}_z\rangle}{\partial\theta}\right)^2} = \frac{1}{t^2}\frac{1}{N}\frac{1}{n(n+1)}\frac{1}{c_2'^2}, \tag{15}$$

where the last equality is evaluated at optimal times such that $c_2 t = k\times 2\pi,\ k\in\mathbb{N}$ (for the detailed derivation and a general formula valid for all times, see Appendix C1). This sensitivity, due to the missing φ'^2 term, does not reach the bound from Eq. (13). We thus conclude that, whenever the θ dependence of c_2 is stronger than the one of φ, most of the information about the parameter is accessible only with the qubit subsystem. The estimation from the measurement of $\hat{J}_z$ is sensitive only to the dynamical qubit-induced phase shift of the mode frequency.

Let us now instead consider the case where the measurement is performed on the photons with the qubit degree of freedom traced out, via the quadrature operator [78,79]

$$\hat{X}_\phi = \tfrac{1}{2}\left(\hat{a}e^{-i(\phi/2)} + \hat{a}^\dagger e^{i(\phi/2)}\right), \tag{16}$$

where ϕ is a phase that can be adjusted to maximize the signal. With the help of Eq. (6) and a coherent state of light at the input with $\eta = 0$, we obtain (see Appendix C2 for details)

$$\Delta^2\theta = \frac{\Delta^2\hat{X}_\phi}{\left(\frac{\partial\langle\hat{X}_\phi\rangle}{\partial\theta}\right)^2} = \frac{1}{t^2}\frac{1}{4n}\frac{1}{\varphi'^2}, \tag{17}$$

again at optimal times $c_2 t = 2\pi k,\ k\in\mathbb{N}$ and with ϕ chosen such that $\sin^2(\varphi + \phi/2) = 1$. We see that a measurement performed on the photons saturates the bound from Eq. (13) if the contribution proportional to c_2 can be neglected. For these optimal times, the estimation of θ with the measurement of quadrature is sensitive only to the static collective shift of the cavity frequency but insensitive to the dynamical shift.

Therefore, given a classical input state of light and matter, by performing the measurement on the qubits one can reach a sensitivity scaling at the Heisenberg limit with the photon number and at the shot-noise limit with the qubit number. If the measurement is performed on the photons, the Heisenberg scaling is achieved with respect to the number of qubits instead. This can be understood by the following reasoning. The estimation by measuring a subsystem is equivalent to averaging out over the remaining parts of the whole system. Since the measured subsystem is described by a classical state, the precision cannot surpass the respective shot-noise limit.

The precision is enhanced due to the collective effects inherent to the Hamiltonian from Eq. (1). However, to reach the double-Heisenberg scaling, as in Eq. (10), one should restore to the simultaneous measurement on both the qubit and the photonic subspace.

III. IMPACT OF CAVITY PUMP AND LOSS

In this section, we consider a more realistic case where the electromagnetic field is coherently driven, later addressing also the impact of the photon loss.

A. Lossless case

Starting from a vacuum state of the photons together with all qubits pointing in the z direction [see Eq. (12)], the state at time t is described by the following density matrix:

$$\hat{\varrho}(t) = \sum_{m,m'} C_m C_{m'} |\gamma_m\rangle\langle\gamma_{m'}| \otimes |m\rangle\langle m'| \times e^{i\eta(\beta_m - \beta_{m'})t} e^{-i[\beta_m^2 \sin(\omega_m t) - \beta_{m'}^2 \sin(\omega_{m'} t)]}, \tag{18}$$

where $|\gamma_m\rangle$ denotes a coherent state of light with the amplitude $\gamma_m = \beta_m(e^{-i\omega_m t} - 1)$, with $\omega_m = -\Delta_c + c_1 N + c_2 m$ and $\beta_m = \eta/\omega_m$ (see Appendix A).

The state of the light, tracing out the subspace of qubits, is a mixture of coherent states

$$\hat{\varrho}_L(t) = \mathrm{Tr}[\hat{\varrho}(t)]_A = \sum_m C_m^2 |\gamma_m\rangle\langle\gamma_m|. \tag{19}$$

We note that the average number of photons is given by

$$n = \langle\hat{n}\rangle = \mathrm{Tr}[\hat{n}\hat{\varrho}_L(t)] = \sum_m C_m^2 |\gamma_m|^2. \tag{20}$$

Depending on the relative strength of the parameters entering the Hamiltonian and the properties of the state of the system, we can specify two different limits: coherent and incoherent regime. Below, we address these in more detail.

1. Coherent regime

For small times, the impact of the dynamical phase shift on the dynamics is negligible. In such a case, ω_m is independent of the state of the matter and is given only by the static shift of the cavity frequency, i.e., $\omega_m \approx \varphi$ [see Eq. (14)]. The requirement is that the following condition

$$|-\Delta_c + c_1 N| \gg |c_2| m \tag{21}$$

is satisfied for all m that significantly contribute to the state in Eq. (18).

The state remains in this coherent regime, as long as the time t is sufficiently short so that the amplitude C_m with maximal m's that significantly contribute to the state, i.e., with $m = \pm\sqrt{N}$, has approximately the same phase. This is true up to $t \simeq \tau_c = \frac{2}{\sqrt{N}|c_2|}$ where the subscript "c" stands for a "collapse." Within this time frame we have $\gamma_m \simeq \gamma = \frac{\eta}{\varphi}(e^{-i\varphi t} - 1)$ for all m and the sum Eq. (19) can be explicitly calculated, giving a pure coherent state of light $\hat{\varrho}_L(t) \simeq |\gamma\rangle\langle\gamma|$. Consequently, the number of photons oscillates as

$$\langle\hat{n}\rangle \simeq |\gamma|^2 = 2\bar{n}\sin^2\left(\frac{\varphi t}{2}\right), \tag{22}$$

where $\bar{n} = 2\frac{\eta^2}{\varphi^2}$ is the number of photons averaged over one period of oscillations of $\langle\hat{n}\rangle$. When the time t exceeds τ_c, contributions to Eq. (20) oscillate out of phase, giving $\langle\hat{n}\rangle \simeq \bar{n}$. Time oscillations of the mean photon number revive when $t \simeq \tau_r = \frac{\pi}{c_2}$, giving a pattern of collapses and revivals, in analogy to the dynamics of a two-level atom within the Jaynes-Cummings model, driven by a monochromatic coherent state of light [78,79].

We now focus on this oscillatory regime and calculate the sensitivity using the estimation strategies discussed in Sec. II B. Let us first consider the measurement of the light quadrature, for which the sensitivity, calculated again with the error propagation formula reads

$$\Delta^2\theta = \frac{\langle(\Delta\hat{X}_\phi)^2\rangle}{\left(\frac{\partial\langle\hat{X}_\phi\rangle}{\partial\theta}\right)^2} \simeq \frac{1}{t^2}\frac{1}{2\bar{n}}\frac{1}{\varphi'^2} \tag{23}$$

with the phase chosen such that $\phi + 2\varphi t = (2k+1)\pi,\ k \in \mathbb{N}$ (see Appendix D for details). We used Eq. (19) to get

$$\langle\hat{X}_\phi\rangle = \mathrm{Re}[\gamma e^{-i(\phi/2)}],\quad \langle(\Delta\hat{X}_\phi)^2\rangle \equiv \langle\hat{X}_\phi^2\rangle - \langle\hat{X}_\phi\rangle^2 = \tfrac{1}{4}, \tag{24}$$

where Re[·] stands for the real part. We see that in the driven case, the measurement of the quadrature in the coherent oscillatory regime gives the same sensitivity as predicted by using an input coherent photon state with amplitude set by η/φ. Here, since $\omega_m \approx \varphi$, the dynamical frequency shift does not significantly modify the state, and the information about the parameter is encoded in the static shift of the cavity frequency.

We now turn to the measurement of the qubits $\hat{J}_z$. We use the Heisenberg equations of motion for the collective spin operators

$$\partial_t \hat{J}_{z/y}(t) = -i[\hat{J}_{z/y}(t), \hat{H}] = \pm c_2 \hat{J}_{y/z}(t)\hat{n}(t). \tag{25}$$

In the oscillatory regime, when light is in a pure coherent state, we approximately replace $\hat{n}(t)$ with the average number of photons, i.e., $\partial_t \hat{J}_{z/y}(t) \simeq \pm c_2 \hat{J}_{y/z}(t)|\gamma|^2$. This gives $\hat{J}_z(t) = \hat{J}_z\cos(\chi) + \hat{J}_y\sin(\chi)$, with

$$\chi \equiv c_2\int_0^t d\tau|\gamma|^2 = \bar{n}[1 - \mathrm{sinc}(\varphi t)]c_2 t. \tag{26}$$

The error propagation formula then yields

$$\Delta^2\theta = \frac{\Delta^2\hat{J}_z(t)}{(\partial_\theta\langle\hat{J}_z(t)\rangle)^2} = \frac{1}{(\chi')^2}\frac{1}{N} \simeq \frac{1}{t^2}\frac{1}{N}\frac{1}{\bar{n}^2}\frac{1}{c_2'^2}, \tag{27}$$

if $|\frac{c_2}{c_2'}\frac{\varphi'}{\varphi}| \ll 1$ and $\mathrm{sinc}(\varphi t) \ll 1$. Note that, although the oscillations of the photonic dynamics revive periodically, the mean-field approximation used above can be safely applied only once. This is because in the long collapse periods, though the dynamics of the photonic population is virtually frozen, the atomic operators undergo a complex dynamics, setting an unknown initial condition for the solution in the next oscillatory regime. Also for this estimation strategy, within the first coherent oscillatory regime the sensitivity form Eq. (27) coincides with the expression from Eq. (15) if the mean number of photons $\bar{n}$ equals the intensity of the coherent state n and $n \gg 1$, so that in Eq. (15), the term $n(n+1)$ can be approximated with n^2.

For times larger than τ_c, the photonic dynamics is frozen so we do not expect the t^{-2} scaling of the sensitivity encountered in the oscillatory case [see Eq. (23)]. Indeed, the mean quadrature and its variance are now

$$\langle\hat{X}_\phi\rangle = -\sqrt{\frac{\bar{n}}{2}}\cos\left(\frac{\phi}{2}\right), \quad \langle(\Delta\hat{X}_\phi)^2\rangle = \frac{1}{4}(\bar{n}+1), \tag{28}$$

thus

$$\Delta^2\theta \simeq \frac{1}{2\bar{n}}\frac{\varphi^2}{\varphi'^2}, \tag{29}$$

when $\bar{n} \gg 1$. Here, the inverse scaling with time as well as with the number of qubits is lost, due to presence of φ^2 in the numerator. For the case where the measurement is performed on the qubits, an analytical calculation similar to that presented in Eqs. (25)–(27) is not possible after τ_c, as light is not in a pure coherent state anymore. Therefore, we must rely on the numerical exact diagonalization of the Hamiltonian from (1) which gives a sensitivity which is orders of magnitude smaller than in the oscillatory regime.

2. Incoherent regime

When the impact of the dynamical phase shift due to the presence of qubits cannot be neglected, the state of the photons cannot be described by a single coherent state. In such a case, when the condition in Eq. (21) is not satisfied, the replacement of the mixture in Eq. (19) with a pure coherent state is not justified at all times, and the mean number of photons is given with the general formula from Eq. (20). The first two moments of the quadrature are now

$$\langle\hat{X}_\phi\rangle = \sum_m C_m^2 \mathrm{Re}[\gamma_m e^{-i(\phi/2)}], \tag{30a}$$

$$\langle\hat{X}_\phi^2\rangle = \sum_m C_m^2 \mathrm{Re}[\gamma_m e^{-i(\phi/2)}]^2 + \frac{1}{4}. \tag{30b}$$

Although one has to resort to numerical simulations in this general case, we show that in the presence of the photon loss, the sensitivity from (23) can be still determined even in the incoherent regime.

B. Impact of photon losses

In this section we include the possibility for photons to be lost from the electromagnetic mode at a rate κ. We do not consider additional effective losses which could come from unwanted coupling between the qubit and other photon modes. The dynamics of the system is then described by the following quantum master equation [83] for the density matrix of the system:

$$\frac{d}{dt}\hat{\varrho} = -i[\hat{H},\hat{\varrho}] + \kappa\left(\hat{a}\hat{\varrho}\hat{a}^\dagger - \frac{1}{2}\{\hat{a}^\dagger\hat{a},\hat{\varrho}\}\right). \tag{31}$$

To proceed, we again separately distinguish the coherent and the incoherent dynamics regime, according to the condition from Eq. (21).

1. Coherent regime

In the coherent regime, when $t \lesssim \tau_c$, we model the photon dynamics by effectively including the loss term in the equation for the coherent amplitude, i.e., $\partial_t\gamma = (-i\varphi - \frac{\kappa}{2})\gamma - i\eta$. With the solution of the photonic state, which is given by

$$\gamma = \frac{\eta}{\varphi - i\frac{\kappa}{2}}(e^{-i\varphi t-(\kappa/2)t} - 1), \tag{32}$$

we determine the mean and the variance of the quadrature by inserting γ from Eq. (32) into Eq. (24). In the short-time limit $\kappa t \ll 1$, we obtain the following sensitivity:

$$\Delta^2\theta \simeq \frac{1}{2\bar{n}_\kappa(\varphi' t)^2}\frac{\varphi^2+\frac{\kappa^2}{4}}{\varphi^2}, \tag{33}$$

where $\bar{n}_\kappa = 2\frac{\eta^2}{\varphi^2+\frac{\kappa^2}{4}}$ is the time-averaged number of photons. In the opposite limit, when $\kappa t \gg 1$, but still $t \lesssim \tau_c$, we have $\gamma \simeq -\frac{\eta}{\varphi - i\frac{\kappa}{2}}$. This gives the sensitivity from the mean quadrature:

$$\Delta^2\theta = \frac{1}{\bar{n}_\kappa\varphi'^2}\frac{\left(\varphi^2+\frac{\kappa^2}{4}\right)^3}{\left(\varphi^2-\frac{\kappa^2}{4}\right)^2}. \tag{34}$$

Similarly to Eq. (29), the presence of φ^2 in the numerator compensates for the scaling of φ'^2 with the number of qubits and thus the collective effect is absent.

Adapting the approach from Eqs. (25)–(27) to the presence of photon loss, we determine the sensitivity from the measurement of $\hat{J}_z(t)$ [see Eq. (26)]:

$$\chi = \frac{1}{2}c_2\bar{n}_\kappa\Bigg[t + \frac{1-e^{-\kappa t}}{\kappa} - \frac{1}{\varphi^2+\frac{\kappa^2}{4}} \times [\kappa - e^{-\kappa t/2}\kappa\cos(\varphi t) + 2e^{-\kappa t/2}\varphi\sin(\varphi t)]\Bigg]. \tag{35}$$

When $\kappa t \ll 1$, the error propagation formula reproduces Eq. (27) with $\bar{n}$ replaced by $\bar{n}_\kappa$, namely,

$$\Delta^2\theta \simeq \frac{1}{t^2}\frac{1}{N}\frac{1}{\bar{n}_\kappa^2}\frac{1}{c_2'^2}. \tag{36}$$

In the limit $\kappa t \to \infty$, we obtain the sensitivity

$$\Delta^2\theta \simeq \frac{1}{t^2}\frac{1}{N}\frac{1}{\bar{n}_\kappa^2}\frac{1}{\left(\frac{a_2'}{2} - \frac{\varphi\varphi'}{\varphi^2+\frac{\kappa^2}{4}}\right)^2}. \tag{37}$$

The solutions presented here are compared with numerical calculations in Figs. 1 and 2. To illustrate the usefulness of the formulas we derived, we take, as the initial state, the vacuum state of the photons together with $N = 20$ qubits pointing in the z direction, and, setting the unit of frequency to $|\Delta_c|$, the other parameters we consider are: $c_1 = -0.5$, $c_2 = -0.2$, $\Delta_c = -1$, $c_1' = c_2' = 1$, $\eta = 8$, and $\kappa = 0.3$, so that both oscillations and collapse are visible. Here, we also assumed for simplicity that θ is dimensionless. In this case, the important timescale is given by $\tau_c|\Delta_c| = 2.24$. Estimation from the mean quadrature agrees perfectly with the analytical expression presented in this section, recovering both collapse and revival. On the other hand, the estimation from the qubits deviates once the initial oscillations are damped, which is when $t > \tau_c$.

The results of Eqs. (33) and (37), show that the collective scalings of the sensitivity with the number of photons and

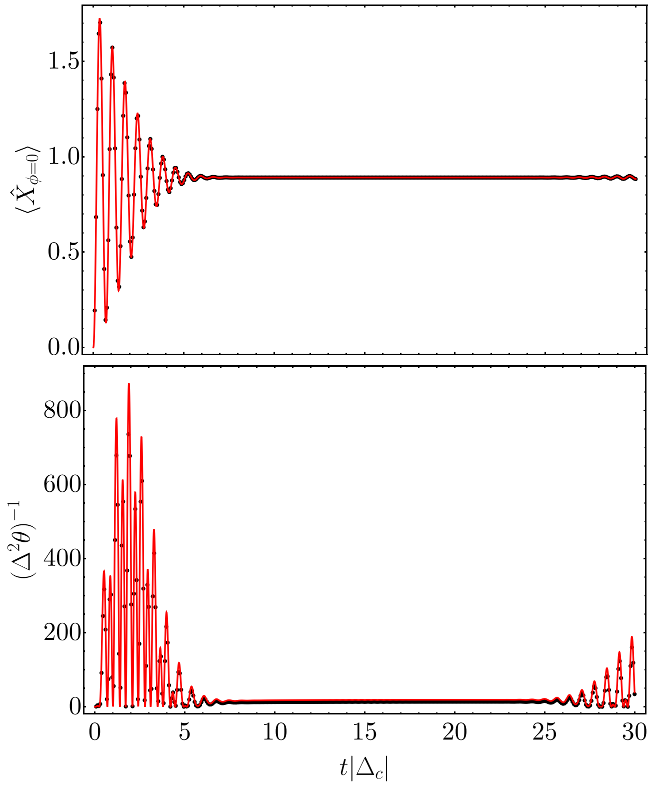

FIG. 1. Dynamics and sensitivity for the photonic subspace. The average value of the quadrature $\hat{X}_\phi$ for $\phi = 0$ (top) and inverse of the error propagation formula (bottom) for quadrature as a function of $t|\Delta_c|$; the axes are in dimensionless units. Black points represent results of numerical calculations, while the red solid line stands for the analytic solution. With the unit of frequency set to $|\Delta_c|$ we consider the following parameters: $N = 20$, $c_1 = -0.5$, $c_2 = -0.2$, $\Delta_c = -1$, $c_1' = c_2' = 1$, $\eta = 8$, and $\kappa = 0.3$, while the initial state consists of a vacuum state of the photons together with all qubits pointing in the z direction.

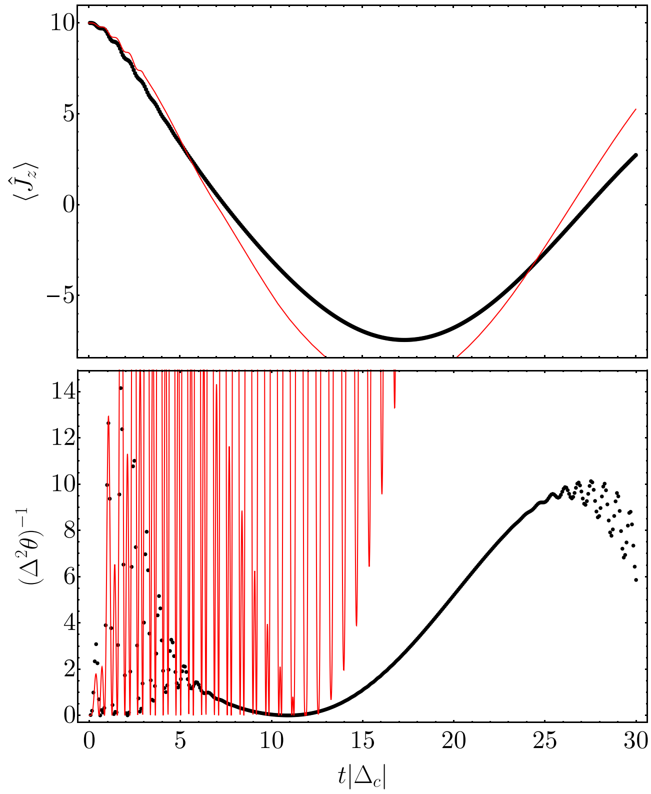

FIG. 2. Dynamics and sensitivity for the qubit subspace. The average value of the operator $\hat{J}_z$ (top) and inverse of the error propagation formula (bottom) for $\hat{J}_z$ as a function of $t|\Delta_c|$; the axes are in dimensionless units. Black points represent results of numerical calculations, while the red solid line stands for the analytic solution valid when $t < \tau_c = 2.24\,|\Delta_c|^{-1}$. Parameters used for calculations are the same as in Fig. 1.

qubits can be retained in the presence of losses for both estimation strategies.

2. *Incoherent regime*

We now turn to the incoherent regime where the condition from (21) does not hold. In this case, we solve the same equation for the coherent amplitude γ_m as above, this time in each subspace of fixed m. We obtain

$$\gamma_m = \frac{\eta}{\omega_m - i\frac{\kappa}{2}}(e^{-i\omega_m t - \kappa t} - 1). \tag{38}$$

Although an analytical expression for the sensitivity is not available in general, a closed formula for $\Delta\theta$ from the quadrature measurement can be found in some regimes, which provides insight into the scalings.

First, taking the limit of large times $\kappa t \gg 1$ and assuming that κ can be neglected in comparison to ω_m for all m, we get $\gamma_m = -\eta/\omega_m$. We can now calculate the mean number of photons using Eq. (20), and similarly the two lowest moments of the quadrature with Eqs. (30), yielding $\langle \hat{X}_\phi \rangle = -\cos(\phi/2)\sum_m C_m^2 \eta/\omega_m$ and $\langle \hat{X}_\phi^2 \rangle = 1/4 + \cos^2(\phi/2)\langle \hat{n} \rangle$. Now, if $\langle \hat{n} \rangle \gg 1$ and $\omega_m \ll \eta$ for those m's where C_m are significantly nonzero, we have $\langle \hat{X}_\phi \rangle \ll \langle \hat{n} \rangle$ and $\langle \hat{X}_\phi^2 \rangle \simeq \cos^2(\phi/2)\langle \hat{n} \rangle$, and thus $\Delta^2\hat{X} \simeq \cos^2(\phi/2)\langle \hat{n} \rangle$. The error propagation formula then yields the shot-noise scaling with the photon number and the enhanced scaling with the number of qubits:

$$\Delta^2\theta = \frac{\langle \hat{n} \rangle}{\left(\sum_m C_m^2 \frac{\eta}{\omega_m^2}\omega_m'\right)^2} \approx \frac{\eta^2}{N^2 c_1'^2 \langle \hat{n} \rangle}, \tag{39}$$

where in the last step we approximated $\omega_m' = c_1' N - c_2' m \approx c_1' N$.

In the next section, we use our results to calculate the sensitivity of the estimation of the gravitational acceleration in a realistic setting.

IV. APPLICATION TO GRAVIMETRY

Here we offer a concrete example where the cooperative enhancement of the sensitivity can be exploited to measure precisely the gravitational acceleration.

Specifically, we consider an optical cavity with resonance frequency ω_c, driven by a laser with a strength η and frequency ω_l, far detuned from an electronic transition of atoms (with resonance frequency ω_a), i.e., $\Delta_a = \omega_l - \omega_a$ is by far

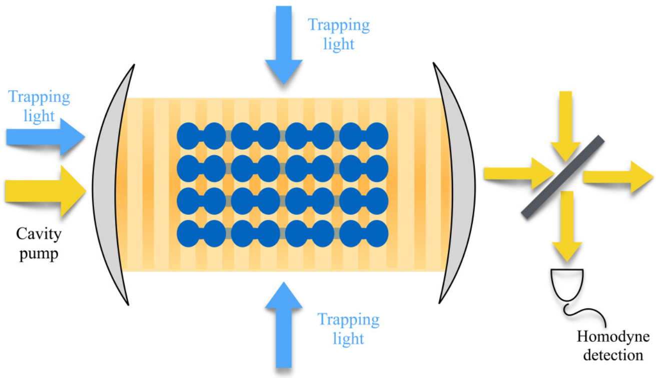

FIG. 3. The scheme of a hybrid light-matter system used as a gravitational sensor. The standing wave (yellow beam) of the cavity formed between two mirrors (gray) modifies the tunneling barrier between the two wells (blue) formed by the trapping light (blue arrows). The cavity is driven by an external laser (see the main text in Sec. IV), and the outgoing light can be analyzed in a homodyne detector.

the largest scale, so that the excited state can be adiabatically eliminated. The atoms are trapped in an optical lattice, which has the same wave vector k as the cavity mode has in the cavity-axis direction. The cavity mode is chosen to be the TEM_{00} with a broad Gaussian envelope in the direction transverse to the cavity axis, such that the transverse spatial variation (with characteristic scale w_0; see below) is negligible over the length of the lattice. The cavity-Hubbard model corresponding to this configuration is derived in [84]. In order to implement an N-qubit Hamiltonian, we include an additional superlattice modulation along the cavity axis and increase the lattice depth in the transverse direction, such to create an array of decoupled double wells, as depicted in Fig. 3. In this case, since the cavity model couples equally to each double well, the system's Hamiltonian simplifies to

$$\hat{H} = \hat{H}_\mathrm{l} + \hat{H}_\mathrm{a} + \hat{H}_\mathrm{a+l}, \tag{40}$$

where

$$\hat{H}_\mathrm{l} = -\Delta_c \hat{n} + \eta(\hat{a} + \hat{a}^\dagger), \tag{41a}$$

$$\hat{H}_\mathrm{a} = \omega_J \hat{J}_x, \tag{41b}$$

$$\hat{H}_\mathrm{a+l} = (U_0 J_0 \hat{N} + 2U_0 J \hat{J}_x)\hat{n}, \tag{41c}$$

where the collective angular momentum operators

$$\hat{J}_x = \frac{1}{2}(\hat{b}_1^\dagger \hat{b}_2 + \hat{b}_2 \hat{b}_1^\dagger), \tag{42a}$$

$$\hat{J}_y = \frac{1}{2i}(\hat{b}_1^\dagger \hat{b}_2 - \hat{b}_2 \hat{b}_1^\dagger), \tag{42b}$$

$$\hat{J}_z = \frac{1}{2}(\hat{b}_1^\dagger \hat{b}_1 - \hat{b}_2^\dagger \hat{b}_2), \tag{42c}$$

are composed of the annihilation operators $\hat{b}_{1,2}$ of the left (right) mode of a double well. The hopping rate within a given double well takes the standard form

$$\omega_J = -2\int dx\, w(x-x_1)\left(-\frac{1}{2m}\frac{d^2}{dx^2} + \cos^2(kx)\right) \times w(x-x_2), \tag{43}$$

with $w(x - x_{1,2})$ being the Wannier-like states localized at the corresponding site of the double well. The atom-cavity coupling constants $U_0 J_0 = c_1$ and $2U_0 J = c_2$ depend on the dispersive shift of the cavity frequency per atom $U_0 = \frac{\Omega_R^2}{\Delta_a}$, where Ω_R is the vacuum Rabi frequency corresponding to the cavity mode, as well as on the overlap integrals

$$J_0 = \int dx |w(x-x_{1,2})|^2 \cos^2(kx) \tag{44}$$

and

$$J = \int dx\, w(x-x_1)\cos^2(kx) w(x-x_2). \tag{45}$$

The linear gravitational potential $V_\mathrm{grav}(x) = mgx$ is directed along the cavity axis (see Fig. 3 for the schematic representation of the setup) and has a twofold impact on the system. First, it modifies the Hamiltonian parameters given by the overlap integrals by shifting the double-well minima $x_{1,2}$, i.e.,

$$w(x - x_{1,2}) \to w(x - x_{1,2} + x_0), \tag{46}$$

where $x_0 = g/\omega_x^2$ and ω_x is the oscillator frequency corresponding to the harmonic part of the potential around a given site of the double well. Second, it adds an energy-imbalance term $\delta \hat{J}_z$ to the Hamiltonian, where

$$\delta = \int dx\, V_\mathrm{grav}(x)[|w(x-x_1)|^2 - |w_2(x-x_2)|^2]. \tag{47}$$

However, for the parameters considered below, δ is small enough for this term to be neglected. We thus see that the setup considered allows one to implement the desired model of Eq. (1).

In order to provide a realistic estimate for the sensitivity of the measurement of g, we use parameters corresponding to the current experiment in Zurich [85]. We take a cavity with finesse $\mathcal{F} = 2.08\times10^5$, length $L = 2.45$ mm, the Gaussian envelope width $w_0 \sim 50\ \mu$m, and loss rate $\kappa = 147\times 2\pi$ kHz. Setting the distance between the wells $D = \lambda/2$, with the wavelength of the cavity mode $\lambda = 785$ nm [85]. By choosing a lattice depth of 57 kHz we get $\omega_x = 2\pi \times 18.2$ kHz. We choose ^{87}Rb atoms and the detuning from the atomic transition $\Delta_a = -1.97$ GHz, which gives $c_1 = -66.6$ kHz and $c_2 = -3.3$ kHz. The derivatives of these two coefficients with respect to parameter x_0 are $c_1' = 3.9\ \frac{\mathrm{GHz}}{\mathrm{m}}$ and $c_2' = 192\frac{\mathrm{MHz}}{\mathrm{m}}$.

With $N \approx 10^6$ atoms, the renormalized cavity detuning φ can be tuned to 9.04 MHz (the bare detuning being $\Delta_c = -66.6$ GHz), giving the mean number of photons $\bar{n} \simeq 137$ for $\eta = 100$ MHz. If $t > 1/\kappa$, and when the input state of atoms is the coherent spin state [see Eq. (12)], the formula from Eq. (39) yields the precision per shot $\Delta g = 6\times10^{-1} g$. Such sensitivity can be reached within a measurement time on the order of κ: $\frac{\Delta g}{g} \sim 6.25\times10^{-4}\frac{1}{\sqrt{\mathrm{Hz}}}$. If we use $N \approx 10^7$ atoms instead, the same setup can be adjusted by changing the bare detuning to $\Delta_c = -666.2$ GHz. The normalized cavity detuning φ is tuned to 25.4 MHz, giving the mean number of photons $\bar{n} \simeq 20$ for $\eta = 100$ MHz. For $t > 1/\kappa$ we obtain then $\Delta g = 2.1\times10^{-1} g$ and $\frac{\Delta g}{g} \sim 2.22\times10^{-4}\frac{1}{\sqrt{\mathrm{Hz}}}$.

In order to make our predictions even more realistic, the model could be refined, most notably including atomic multimode effects and limitations in the detection efficiency. At this stage we can already claim that the protocol considered should be less sensitive to these effects than protocols relying on reaching the genuine, i.e., entanglement based, Heisenberg scaling [86].

V. CONCLUSIONS

We have shown that a hybrid system of matter and light can act as a sensing device in which the cooperative effects play a prominent role. These effects generically enhance the precision by improving the scaling with the number of particles in both subsystems.

By considering a fundamental model of N qubits coupled to a single electromagnetic mode, we showed that the precision in estimating the light-matter coupling constant exhibits a double-Heisenberg scaling $\Delta\theta \propto 1/(Nn)$, where n is the number of photons. This scaling requires the use of an entangled state of matter or a nonclassical state of photons. However, even for classical states a Heisenberg scaling with the number of qubits or photons can be reached.

To illustrate the usefulness of our hybrid light-matter sensor, we proposed a specific, experimentally feasible scheme in which a Bose-Einstein condensate is trapped in a double-well optical lattice within an optical cavity. We predicted that, even taking into account photon loss, the sensor can potentially determine the gravitational acceleration g with a relative precision reaching $\frac{\Delta g}{g} \sim 2.22\times10^{-4}\ \mathrm{Hz}^{-1/2}$. Such a precision can still be improved by employing nonclassical states of matter and light.

ACKNOWLEDGMENT

A.N. and J.C. are supported by Project No. 2017/25/Z/ST2/03039, funded by the National Science Centre, Poland, under the QuantERA program.

APPENDIX A: EVOLUTION OPERATOR

We now derive the expression for the evolution operator. The Hamiltonian from Eq. (1) can be written as

$$\hat{H} = \hat{\omega}\hat{a}^\dagger\hat{a} + \eta(\hat{a} + \hat{a}^\dagger), \tag{A1}$$

where $\hat{\omega} = c_1N - \Delta_c + c_2\hat{J}_x$. Now we observe that

$$\hat{H} = \hat{\omega}\hat{D}^\dagger(\hat{\beta})\hat{a}^\dagger\hat{a}\hat{D}(\hat{\beta}) - \eta\hat{\beta}, \tag{A2}$$

where $\hat{\beta} = \eta\hat{\omega}^{-1}$, while

$$\hat{D}(\hat{\beta}) = e^{\hat{\beta}\hat{a}^\dagger - \hat{\beta}^\dagger\hat{a}} \tag{A3}$$

is the generalized displacement operator. Since $[\hat{\omega}, \hat{\beta}] = 0$, we can write the evolution operator as follows:

$$\hat{U}(t) = \hat{D}^\dagger(\hat{\beta})e^{-i\hat{\omega}t\hat{a}^\dagger\hat{a}}\hat{D}(\hat{\beta})e^{i\eta t\hat{\beta}}. \tag{A4}$$

The initial state has a general form

$$\hat{\varrho}(0) = \sum_{n,n'=0}^{\infty}\sum_{m,m'=-(N/2)}^{N/2} \varrho_{nn'}^{mm'}|n, m\rangle\langle n', m'|, \tag{A5}$$

where $|n, m\rangle$ denoted a photonic Fock state and an eigenstate of the atomic operator $\hat{J}_x$, namely,

$$|n, m\rangle = |n\rangle \otimes |m\rangle, \quad \hat{a}^\dagger\hat{a}|n\rangle = n|n\rangle, \quad \hat{J}_x|m\rangle = m|m\rangle. \tag{A6}$$

The action of the evolution operator (A4) on the density matrix from Eq. (A5) gives

$$\hat{\varrho}(t) = \sum_{\substack{n,n'\\ m,m'}} \varrho_{nn'}^{mm'}\hat{D}^\dagger(\beta_m)e^{-i\omega_m t\hat{a}^\dagger\hat{a}}\hat{D}(\beta_m)e^{i\eta(\beta_m-\beta_{m'})t} \times |n, m\rangle\langle n', m'|\hat{D}^\dagger(\beta_{m'})e^{i\omega_{m'}t\hat{a}^\dagger\hat{a}}\hat{D}(\beta_{m'}), \tag{A7}$$

where $\gamma_m = \beta_m(e^{-i\omega_m t} - 1)$, $\omega_m = -\Delta_c + c_1N + c_2m$, and $\beta_m = \frac{\eta}{\omega_m}$. Note that

$$|\Phi_1\rangle \equiv \hat{D}(\beta)|n\rangle = \frac{1}{\sqrt{n!}}\hat{D}(\beta)(\hat{a}^\dagger)^n|0\rangle \times \frac{1}{\sqrt{n!}}\hat{D}(\beta)(\hat{a}^\dagger)^n\hat{D}^\dagger(\beta)\hat{D}(\beta)|0\rangle = \frac{1}{\sqrt{n!}}(\hat{a}^\dagger - \beta)^n|\beta\rangle, \tag{A8}$$

as $\beta \in \mathbb{R}$. With this expression at hand, we can take the next step and act with the free-evolution term

$$\begin{aligned}|\Phi_2\rangle \equiv e^{-i\omega\hat{a}^\dagger\hat{a}t}|\Phi_1\rangle &= \frac{1}{\sqrt{n!}}e^{-i\omega\hat{a}^\dagger\hat{a}t}(\hat{a}^\dagger - \beta)^n|\beta\rangle\\ &= \frac{1}{\sqrt{n!}}e^{-i\omega\hat{a}^\dagger\hat{a}t}(\hat{a}^\dagger - \beta)^n e^{i\omega\hat{a}^\dagger\hat{a}t}e^{-i\omega\hat{a}^\dagger\hat{a}t}|\beta\rangle\\ &= \frac{1}{\sqrt{n!}}(\hat{a}^\dagger e^{-i\omega t} - \beta)^n|\beta e^{-i\omega t}\rangle.\end{aligned} \tag{A9}$$

In the last step, we add the second displacement operator, to get

$$\begin{aligned}\hat{D}^\dagger(\beta)|\Phi_2\rangle &= \frac{1}{\sqrt{n!}}\hat{D}^\dagger(\beta)(\hat{a}^\dagger e^{-i\omega t} - \beta)^n|\beta e^{-i\omega t}\rangle\\ &= \frac{1}{\sqrt{n!}}\hat{D}^\dagger(\beta)(\hat{a}^\dagger e^{-i\omega t} - \beta)^n\hat{D}(\beta)\hat{D}^\dagger(\beta)|\beta e^{-i\omega t}\rangle\\ &= \frac{1}{\sqrt{n!}}e^{-i\beta^2\sin(\omega t)}[(\hat{a}^\dagger + \beta)e^{-i\omega t} - \beta]^n|\beta e^{-i\omega t} - \beta\rangle\\ &= \frac{1}{\sqrt{n!}}e^{-i\beta^2\sin(\omega t)}(\hat{a}^\dagger e^{-i\omega t} + \gamma)^n|\gamma\rangle,\end{aligned} \tag{A10}$$

where $\gamma = \beta(e^{-i\omega t} - 1)$. We again use the displacement operator

$$\begin{aligned}(\hat{a}^\dagger e^{-i\omega t} + \gamma)^n|\gamma\rangle &= \frac{1}{\sqrt{n!}}(\hat{a}^\dagger e^{-i\omega t} + \gamma)^n\hat{D}(\gamma)|0\rangle\\ &= \hat{D}(\gamma)\hat{D}^\dagger(\gamma)(\hat{a}^\dagger e^{-i\omega t} + \gamma)^n\hat{D}(\gamma)|0\rangle\\ &= \hat{D}(\gamma)[(\hat{a}^\dagger + \gamma^*)e^{-i\omega t} + \gamma]^n|0\rangle.\end{aligned} \tag{A11}$$

But note that

$$\begin{aligned}\gamma^* e^{-i\omega t} + \gamma &= \beta(e^{i\omega t} - 1)e^{-i\omega t} + \gamma\\ &= \beta(1 - e^{-i\omega t}) + \gamma = -\gamma + \gamma = 0.\end{aligned} \tag{A12}$$

Therefore, we obtain the final expression

$$\hat{D}^\dagger(\beta)e^{-i\omega\hat{a}^\dagger\hat{a}t}\hat{D}(\beta)|n\rangle = \frac{e^{i\beta^2\sin(\omega t)}}{\sqrt{n!}}\hat{D}(\gamma)(\hat{a}^\dagger e^{-i\omega t})^n|0\rangle = e^{-in\omega t}e^{-i\beta^2\sin(\omega t)}\hat{D}(\gamma)|n\rangle. \quad \text{(A13)}$$

We now plug this result into Eq. (A7) and obtain

$$\hat{\varrho}(t) = \sum_{m,m'} C_m C_{m'}|\gamma_m\rangle\langle\gamma_{m'}| \otimes |m\rangle\langle m'| \times e^{i\eta(\beta_m-\beta_{m'})t}e^{-i[\beta_m^2\sin(\omega_m t)-\beta_{m'}^2\sin(\omega_{m'}t)]} \quad \text{(A14)}$$

as used in the main text.

APPENDIX B: DERIVATION OF THE GENERATOR $\hat{h}$ FROM EQ. (7)

The generator of the interferometric or metrological transformation is equal to

$$\hat{h} = i(\partial_\theta\hat{U})\hat{U}^\dagger. \quad \text{(B1)}$$

The derivative over the parameter will hit all the parameter-dependent parts of the evolution operator. For instance,

$$\partial_\theta\hat{\beta} = -\eta\hat{\omega}^{-2}\frac{\partial\hat{\omega}}{\partial\theta} = -\frac{\hat{\beta}^2}{\eta}\frac{\partial\hat{\omega}}{\partial\theta}. \quad \text{(B2)}$$

All other steps leading to Eq. (7) follow immediately from the properties of the displacement operator.

APPENDIX C: SENSITIVITIES IN THE $\eta = 0$ CASE

We now separately consider the no-pump case where initially light is in a coherent state $|\alpha\rangle$, and derive the expressions for the error propagation formula for atoms and photons only. The complete density matrix in such case is given by

$$\hat{\varrho}(t) = \sum_{m,m'} \varrho_{m,m'}^{(A)}|\gamma_m\rangle\langle\gamma_{m'}| \otimes |m\rangle\langle m'|, \quad \text{(C1)}$$

where $\gamma_m = \alpha e^{-i\omega_m t}$ [note that $\varrho_{m,m'}^{(A)} = C_m C_{m'}$, so $\hat{\varrho}(t)$ is pure]. However, the density-matrix representation is useful for the calculation of the reduced matrices. This is the starting point for the discussion in the remaining part of this Appendix.

1. Error propagation formula for atoms

We first calculate the atomic density matrix by tracing out the photonic degree of freedom. We obtain

$$\hat{\varrho}_A = \text{Tr}[\hat{\varrho}(t)]_L = \sum_{m,m'=0}^{N} \varrho_{m,m'}^{(A)}\langle\gamma_{m'}|\gamma_m\rangle|m\rangle\langle m'| = \sum_{m,m'=0}^{N} \varrho_{m,m'}^{(A)}e^{-\alpha^2\{1-\cos[\delta(m-m')]\}} \times e^{i\alpha^2\sin[\delta(m-m')]}|m\rangle\langle m'|, \quad \text{(C2)}$$

where $\delta = c_2 t$. To calculate the error propagation formula, we note that

$$\hat{J}_z|m\rangle = \frac{1}{2}\left[\sqrt{\left(\frac{N}{2}+m+1\right)\left(\frac{N}{2}-m\right)}|m+1\rangle + \sqrt{\left(\frac{N}{2}+m\right)\left(\frac{N}{2}-m+1\right)}|m-1\rangle\right] \quad \text{(C3)}$$

and analogically for $\hat{J}_z^2$. Therefore we obtain

$$\langle\hat{J}_z\rangle = \frac{N}{2}e^{n(\cos\delta-1)}\cos(n\sin\delta), \quad \text{(C4a)}$$

$$\langle\hat{J}_z^2\rangle = \frac{N}{8}(N-1)[e^{n(\cos 2\delta-1)}\cos(n\sin 2\delta)+1] + \frac{N}{4}, \quad \text{(C4b)}$$

$$\partial_\theta\langle\hat{J}_z\rangle = -\frac{N}{2}nc_2' t e^{n(\cos\delta-1)}\sin[\delta+n\sin\delta]. \quad \text{(C4c)}$$

These expressions, plugged into the error propagation formula (15) give

$$\Delta^2\theta = \frac{1}{Nn^2(c_2' t)^2}\frac{\Delta^2\hat{J}_z}{\frac{1}{4}e^{2n(\cos\delta-1)}\sin^2[\delta+n\sin\delta]}. \quad \text{(C5)}$$

This can be optimized by setting $\delta = k\times 2\pi,\ k \in \mathbb{N}$, which gives Eq. (15).

2. Error propagation formula for photons

We now take the state from Eq. (C1) and trace out the atomic degree of freedom to obtain

$$\hat{\varrho}_L = \text{Tr}[\hat{\varrho}(t)]_A = \sum_{m=0}^{N} \varrho_{m,m}^{(A)}|\gamma_m\rangle\langle\gamma_m|, \quad \text{(C6)}$$

i.e., the state is an incoherent mixture of coherent states. From this representation of the photonic state, we immediately obtain

$$\langle\hat{X}\rangle = \frac{1}{2}\sum_m C_m^2\left(\gamma_m e^{-i(\phi/2)} + \gamma_m^* e^{i(\phi/2)}\right) = \frac{\alpha}{2}\sum_m C_m^2\left(e^{-i[\omega_m t+(\phi/2)]} + \gamma_m^* e^{i[\omega_m t+(\phi/2)]}\right) = \alpha\cos\left(\varphi t + \frac{\phi}{2}\right)\cos^N\left(\frac{\delta}{2}\right), \quad \text{(C7)}$$

where in the last step we used the explicit expression for C_m from Eq. (12). In a similar fashion, we obtain

$$\langle\hat{X}^2\rangle = \frac{1}{4} + \sum_m C_m^2\left(\gamma_m^2 e^{-i\phi} + \gamma_m^{*2}e^{i\phi} + 2|\gamma_m|^2\right) = \frac{1}{4} + \frac{\alpha^2}{2} + \frac{\alpha^2}{2}\cos(2\varphi t + \phi)\cos^N(\delta) \quad \text{(C8)}$$

for the mean of its square.

From these two results, the variance of $\hat{X}$ can be obtained and minimized with respect to δ. By picking $\delta = k\times 2\pi,\ k \in \mathbb{N}$, we obtain

$$\langle(\Delta\hat{X})^2\rangle = \tfrac{1}{4} \quad \text{(C9)}$$

and the error propagation formula gives the sensitivity equal to

$$\Delta^2\theta = \frac{1}{t^2}\frac{1}{4n}\frac{1}{\varphi'^2\sin^2(\varphi+\phi/2)}. \quad \text{(C10)}$$

Once we set $\sin^2(\varphi+\phi/2) = 1$, we recover Eq. (C10).

APPENDIX D: SENSITIVITIES FOR $\eta \neq 0$

The photonic quadrature is

$$\hat{X}_\phi = \frac{1}{2}\left(\hat{a}e^{-i(\phi/2)} + \hat{a}^\dagger e^{i(\phi/2)}\right), \tag{D1}$$

and using Eq. (30) and Eq. (A14) we obtain the mean and the mean square

$$\langle \hat{X}_\phi \rangle = \sum_m C_m^2 \frac{\eta}{\omega_m}\left[\cos\left(\omega_m t + \frac{\phi}{2}\right) - \cos\left(\frac{\phi}{2}\right)\right], \tag{D2a}$$

$$\langle \hat{X}_\phi^2 \rangle = \sum_m C_m^2 \frac{\eta^2}{\omega_m^2}\left[\cos\left(\omega_m t + \frac{\phi}{2}\right) - \cos\left(\frac{\phi}{2}\right)\right]^2 + \frac{1}{4}. \tag{D2b}$$

In the oscillatory regime and when the approximation from (21) holds, the dependence of ω_m on m can be dropped, giving

$$\langle \hat{X}_\phi \rangle \simeq \left[\cos\left(\varphi t + \frac{\phi}{2}\right) - \cos\left(\frac{\phi}{2}\right)\right]\frac{\eta}{\varphi}. \tag{D3a}$$

$$\langle \hat{X}_\phi^2 \rangle \simeq \langle \hat{X}_\phi \rangle^2 + \frac{1}{4}. \tag{D3b}$$

The sensitivity is inversely proportional to the square of the derivative of $\langle \hat{X}_\phi \rangle$, equal to

$$\frac{\partial \langle \hat{X}_\phi \rangle}{\partial \theta} = -\frac{\eta}{\varphi^2}\varphi'\left[\cos\left(\varphi t + \frac{\phi}{2}\right) - \cos\left(\frac{\phi}{2}\right) + \sin\left(\varphi t + \frac{\phi}{2}\right)\varphi t\right], \tag{D4}$$

thus by choosing ϕ in such a way that $\varphi t + \frac{\phi}{2} = \frac{\pi}{2} + k\pi,\ k \in \mathbb{N}$, we obtain

$$\Delta^2\theta \simeq \frac{1}{t^2}\frac{1}{2\bar{n}}\frac{1}{\varphi'^2}. \tag{D5}$$

For atoms, the mean-field approximation described in the main text gives with

$$\Delta^2\theta = \frac{\Delta^2 \hat{J}_z(t)}{(\partial_\theta \langle \hat{J}_z(t)\rangle)^2} = \frac{1}{N}\frac{1}{(\chi')^2}, \tag{D6}$$

where

$$\chi(t) = c_2 \int_0^t d\tau\, |\gamma|^2 = 2c_2 t \frac{\eta^2}{\varphi^2}[1 - \mathrm{sinc}(\varphi t)]. \tag{D7}$$

For those sufficiently late instants of time t, when $\mathrm{sinc}(\varphi t) \ll 1$, the error propagation formula gives

$$\Delta^2\theta = \frac{\Delta^2 \hat{J}_z(t)}{(\partial_\theta \langle \hat{J}_z(t)\rangle)^2} = \frac{1}{t^2}\frac{1}{N}\frac{1}{\bar{n}^2}\frac{1}{(c_2')^2}\frac{1}{\left(1 - 2\frac{c_2}{c_2'}\frac{\varphi'}{\varphi}\right)^2}. \tag{D8}$$

In the collapse regime, the cosine functions cancel out in Eqs. (D2), while the cosine squared averages to $1/2$, giving

$$\langle \hat{X}_\phi \rangle \simeq -\frac{\eta}{\varphi}\cos\left(\frac{\phi}{2}\right), \tag{D9a}$$

$$\langle \hat{X}_\phi^2 \rangle \simeq \frac{\eta^2}{\varphi^2}\left[\frac{1}{2} + \cos^2\left(\frac{\phi}{2}\right)\right] + \frac{1}{4}. \tag{D9b}$$

The variance is bigger than in the oscillatory regime and the mean grows with time. The sensitivity at $\phi = 0$ is

$$\Delta^2\theta = \frac{\frac{1}{2}\frac{\eta^2}{\varphi^2} + \frac{1}{4}}{\frac{\eta^4}{\varphi^4}\frac{\varphi'^2}{\varphi^2}} \simeq \frac{1}{\bar{n}\frac{\varphi'^2}{\varphi^2}}, \tag{D10}$$

which is $2t^2\varphi^2$ worse than Eq. (D5).

[1] H. Kimble, Nature (London) **453**, 1023 (2008).
[2] S. Ritter, C. Nölleke, C. Hahn, A. Reiserer, A. Neuzner, M. Uphoff, M. Mücke, E. Figueroa, J. Bochmann, and G. Rempe, Nature (London) **484**, 195 (2012).
[3] J. I. Cirac, P. Zoller, H. J. Kimble, and H. Mabuchi, Phys. Rev. Lett. **78**, 3221 (1997).
[4] M. Aspelmeyer, T. J. Kippenberg, and F. Marquardt, Rev. Mod. Phys. **86**, 1391 (2014).
[5] M. Aspelmeyer, P. Meystre, and K. Schwab, Phys. Today **65**(7), 29 (2012).
[6] C. M. Caves, Phys. Rev. Lett. **45**, 75 (1980).
[7] P. Meystre, J. D. McCullen, E. Vignes, and E. M. Wright, J. Opt. Soc. Am. B **2**, 1830 (1985).
[8] V. B. Braginsky and F. Y. Khalili, Rev. Mod. Phys. **68**, 1 (1996).
[9] A. A. Clerk, M. H. Devoret, S. M. Girvin, F. Marquardt, and R. J. Schoelkopf, Rev. Mod. Phys. **82**, 1155 (2010).
[10] A. Schliesser, O. Arcizet, R. Riviere, G. Anetsberger, and T. J. Kippenberg, Nat. Phys. **5**, 509 (2009).
[11] J. Suh, A. J. Weinstein, C. U. Lei, E. E. Wollman, S. K. Steinke, P. Meystre, A. A. Clerk, and K. C. Schwab, Science **344**, 1262 (2014).
[12] H. J. Kimble, Phys. Scr. **1998**, 127 (1998).
[13] J. M. Raimond, M. Brune, and S. Haroche, Rev. Mod. Phys. **73**, 565 (2001).
[14] H. Mabuchi and A. C. Doherty, Science **298**, 1372 (2002).
[15] E. Pedrozo-Peñafiel, S. Colombo, C. Shu, A. F. Adiyatullin, Z. Li, E. Mendez, B. Braverman, A. Kawasaki, D. Akamatsu, Y. Xiao *et al.*, Nature (London) **588**, 414 (2020).
[16] A. Shankar, L. Salvi, M. L. Chiofalo, N. Poli, and M. J. Holland, Quantum Sci. Technol. **4**, 045010 (2019).
[17] L. Salvi, N. Poli, V. Vuletić, and G. M. Tino, Phys. Rev. Lett. **120**, 033601 (2018).
[18] O. Hosten, N. J. Engelsen, R. Krishnakumar, and M. A. Kasevich, Nature (London) **529**, 505 (2016).
[19] R. J. Sewell, M. Koschorreck, M. Napolitano, B. Dubost, N. Behbood, and M. W. Mitchell, Phys. Rev. Lett. **109**, 253605 (2012).
[20] A. Louchet-Chauvet, J. Appel, J. J. Renema, D. Oblak, N. Kjaergaard, and E. S. Polzik, New J. Phys. **12**, 065032 (2010).
[21] J. Appel, P. J. Windpassinger, D. Oblak, U. B. Hoff, N. Kjærgaard, and E. S. Polzik, Proc. Natl. Acad. Sci. USA **106**, 10960 (2009).

[22] J. Hald, J. L. Sørensen, C. Schori, and E. S. Polzik, Phys. Rev. Lett. **83**, 1319 (1999).
[23] I. Teper, G. Vrijsen, J. Lee, and M. A. Kasevich, Phys. Rev. A **78**, 051803(R) (2008).
[24] K. Hammerer, A. S. Sørensen, and E. S. Polzik, Rev. Mod. Phys. **82**, 1041 (2010).
[25] I. D. Leroux, M. H. Schleier-Smith, and V. Vuletić, Phys. Rev. Lett. **104**, 073602 (2010).
[26] Z. Chen, J. G. Bohnet, S. R. Sankar, J. Dai, and J. K. Thompson, Phys. Rev. Lett. **106**, 133601 (2011).
[27] S. Brakhane, W. Alt, T. Kampschulte, M. Martinez-Dorantes, R. Reimann, S. Yoon, A. Widera, and D. Meschede, Phys. Rev. Lett. **109**, 173601 (2012).
[28] F. Haas, J. Volz, R. Gehr, J. Reichel, and J. Estève, Science **344**, 180 (2014).
[29] F. Anders, A. Idel, P. Feldmann, D. Bondarenko, S. Loriani, K. Lange, J. Peise, M. Gersemann, B. Meyer, S. Abend *et al.*, arXiv:2010.15796.
[30] S. S. Szigeti, S. P. Nolan, J. D. Close, and S. A. Haine, Phys. Rev. Lett. **125**, 100402 (2020).
[31] X.-Y. Luo, Y.-Q. Zou, L.-N. Wu, Q. Liu, M.-F. Han, M. K. Tey, and L. You, Science **355**, 620 (2017).
[32] S. S. Szigeti, R. J. Lewis-Swan, and S. A. Haine, Phys. Rev. Lett. **118**, 150401 (2017).
[33] D. Linnemann, H. Strobel, W. Muessel, J. Schulz, R. J. Lewis-Swan, K. V. Kheruntsyan, and M. K. Oberthaler, Phys. Rev. Lett. **117**, 013001 (2016).
[34] I. Kruse, K. Lange, J. Peise, B. Lücke, L. Pezzè, J. Arlt, W. Ertmer, C. Lisdat, L. Santos, A. Smerzi, and C. Klempt, Phys. Rev. Lett. **117**, 143004 (2016).
[35] W. Muessel, H. Strobel, D. Linnemann, T. Zibold, B. Juliá-Díaz, and M. K. Oberthaler, Phys. Rev. A **92**, 023603 (2015).
[36] J. Esteve, C. Gross, A. Weller, S. Giovanazzi, and M. Oberthaler, Nature **455**, 1216 (2008).
[37] C. Gross, T. Zibold, E. Nicklas, J. Esteve, and M. K. Oberthaler, Nature **464**, 1165 (2010).
[38] M. F. Riedel, P. Böhi, Y. Li, T. W. Hänsch, A. Sinatra, and P. Treutlein, Nature **464**, 1170 (2010).
[39] T. Berrada, S. van Frank, R. Bücker, T. Schumm, J.-F. Schaff, and J. Schmiedmayer, Nat. Commun. **4**, 2077 (2013).
[40] A. Perrin, H. Chang, V. Krachmalnicoff, M. Schellekens, D. Boiron, A. Aspect, and C. I. Westbrook, Phys. Rev. Lett. **99**, 150405 (2007).
[41] B. Lücke, M. Scherer, J. Kruse, L. Pezzé, F. Deuretzbacher, P. Hyllus, J. Peise, W. Ertmer, J. Arlt, L. Santos *et al.*, Science **334**, 773 (2011).
[42] R. Bücker, J. Grond, S. Manz, T. Berrada, T. Betz, C. Koller, U. Hohenester, T. Schumm, A. Perrin, and J. Schmiedmayer, Nat. Phys. **7**, 608 (2011).
[43] K. V. Kheruntsyan, J.-C. Jaskula, P. Deuar, M. Bonneau, G. B. Partridge, J. Ruaudel, R. Lopes, D. Boiron, and C. I. Westbrook, Phys. Rev. Lett. **108**, 260401 (2012).
[44] M. Bonneau, J. Ruaudel, R. Lopes, J.-C. Jaskula, A. Aspect, D. Boiron, and C. I. Westbrook, Phys. Rev. A **87**, 061603(R) (2013).
[45] H. Strobel, W. Muessel, D. Linnemann, T. Zibold, D. B. Hume, L. Pezzé, A. Smerzi, and M. K. Oberthaler, Science **345**, 424 (2014).
[46] D. K. Shin, B. M. Henson, S. S. Hodgman, T. Wasak, J. Chwedeńczuk, and A. G. Truscott, Nat. Commun. **10**, 4447 (2019).
[47] V. Giovannetti, S. Lloyd, and L. Maccone, Science **306**, 1330 (2004).
[48] S. S. Szigeti, O. Hosten, and S. A. Haine, Appl. Phys. Lett. **118**, 140501 (2021).
[49] L. Pezzè, A. Smerzi, M. K. Oberthaler, R. Schmied, and P. Treutlein, Rev. Mod. Phys. **90**, 035005 (2018).
[50] A. Wicht, K. Danzmann, M. Fleischhauer, M. Scully, G. Müller, and R.-H. Rinkleff, Opt. Commun. **134**, 431 (1997).
[51] G. S. Pati, M. Salit, K. Salit, and M. S. Shahriar, Phys. Rev. Lett. **99**, 133601 (2007).
[52] D.-W. Wang and M. O. Scully, Phys. Rev. Lett. **113**, 083601 (2014).
[53] J. M. Weiner, K. C. Cox, J. G. Bohnet, Z. Chen, and J. K. Thompson, Appl. Phys. Lett. **101**, 261107 (2012).
[54] J. G. Bohnet, Z. Chen, J. M. Weiner, K. C. Cox, and J. K. Thompson, Phys. Rev. A **88**, 013826 (2013).
[55] K. Gietka, T. Wasak, J. Chwedeńczuk, F. Piazza, and H. Ritsch, Eur. Phys. J. D **71**, 273 (2017).
[56] S. A. Haine, Phys. Rev. Lett. **110**, 053002 (2013).
[57] S. S. Szigeti, B. Tonekaboni, W. Y. S. Lau, S. N. Hood, and S. A. Haine, Phys. Rev. A **90**, 063630 (2014).
[58] S. A. Haine, S. S. Szigeti, M. D. Lang, and C. M. Caves, Phys. Rev. A **91**, 041802(R) (2015).
[59] S. A. Haine and W. Y. S. Lau, Phys. Rev. A **93**, 023607 (2016).
[60] D. Budker and M. Romalis, Nat. Phys. **3**, 227 (2007).
[61] F. Wolfgramm, A. Cerè, F. A. Beduini, A. Predojević, M. Koschorreck, and M. W. Mitchell, Phys. Rev. Lett. **105**, 053601 (2010).
[62] M. Napolitano, M. Koschorreck, B. Dubost, N. Behbood, R. J. Sewell, and M. W. Mitchell, Nature (London) **471**, 486 (2011).
[63] P. R. Berman, *Atom Interferometry* (Academic Press, New York, 1997).
[64] A. D. Cronin, J. Schmiedmayer, and D. E. Pritchard, Rev. Mod. Phys. **81**, 1051 (2009).
[65] F. Sorrentino, K. Bongs, P. Bouyer, L. Cacciapuoti, M. de Angelis, H. Dittus, W. Ertmer, A. Giorgini, J. Hartwig, M. Hauth *et al.*, Microg. Sci. Technol. **22**, 551 (2010).
[66] R. Geiger, A. Landragin, S. Merlet, and F. Pereira Dos Santos, AVS Quantum Sci. **2**, 024702 (2020).
[67] K. Bongs, M. Holynski, J. Vovrosh, P. Bouyer, G. Condon, E. Rasel, C. Schubert, W. P. Schleich, and A. Roura, Nat. Rev. Phys. **1**, 731 (2019).
[68] P. Hamilton, M. Jaffe, J. M. Brown, L. Maisenbacher, B. Estey, and H. Müller, Phys. Rev. Lett. **114**, 100405 (2015).
[69] B. M. Peden, D. Meiser, M. L. Chiofalo, and M. J. Holland, Phys. Rev. A **80**, 043803 (2009).
[70] J. Goldwin, B. P. Venkatesh, and D. H. J. O'Dell, Phys. Rev. Lett. **113**, 073003 (2014).
[71] F. Mivehvar, S. Ostermann, F. Piazza, and H. Ritsch, Phys. Rev. Lett. **120**, 123601 (2018).
[72] K. Gietka, F. Mivehvar, and H. Ritsch, Phys. Rev. Lett. **122**, 190801 (2019).
[73] R. J. Lewis-Swan, D. Barberena, J. A. Muniz, J. R. K. Cline, D. Young, J. K. Thompson, and A. M. Rey, Phys. Rev. Lett. **124**, 193602 (2020).

[74] J. Johansson, P. Nation, and F. Nori, Comput. Phys. Commun. **184**, 1234 (2013).

[75] G. Szirmai, G. Mazzarella, and L. Salasnich, Phys. Rev. A **91**, 023601 (2015).

[76] A. Holevo, *Probabilistic and Statistical Aspects of Quantum Theory* (Publications of Scuola Normale Superiore, 2011).

[77] S. L. Braunstein and C. M. Caves, Phys. Rev. Lett. **72**, 3439 (1994).

[78] C. Gerry and P. Knight, *Introductory Quantum Optics* (Cambridge University Press, Cambridge, UK, 2004).

[79] M. O. Scully and M. S. Zubairy, *Quantum Optics* (Cambridge University Press, Cambridge, UK, 1999).

[80] L. Pezzé and A. Smerzi, Phys. Rev. Lett. **102**, 100401 (2009).

[81] E. C. G. Sudarshan, Phys. Rev. Lett. **10**, 277 (1963).

[82] R. J. Glauber, Phys. Rev. **131**, 2766 (1963).

[83] H.-P. Breuer and F. Petruccione, *The Theory of Open Quantum Systems* (Oxford University Press on Demand, 2002).

[84] C. Maschler, I. B. Mekhov, and H. Ritsch, Eur. Phys. J. D **46**, 545 (2008).

[85] J. Léonard, A. Morales, P. Zupancic, T. Esslinger, and T. Donner, Nature (London) **543**, 87 (2017).

[86] R. Demkowicz-Dobrzański, J. Kołodyński, and M. Guta, Nat. Commun. **3**, 1063 (2012).